*Research Paper*
*Computational Methods for Differential Equations*
http://cmde.tabrizu.ac.ir
Vol. *, No. *, *, pp. 1-18
DOI:10.22034/cmde.2026.70850.3542

# Option Pricing under the Heston Model Using Generalized Gaussian Radial Basis Functions with Variable Shape Parameters

**Nazanin Tafakhori[1], Mojtaba Ranjbar[2,*] and Seyed Mohammad Mahdi Kazemi[2]**

[1]Department of Mathematics, Azarbaijan Shahid Madani University, Tabriz, Iran.

[2]Department of Financial Mathematics, Faculty of Financial Sciences, Kharazmi University, P.O. Box 15936-56311, Tehran, Iran.

**Abstract**

This work offers a new numerical method for solving the Heston stochastic volatility equation used for European and American option pricing problems through radial basis function (RBF) collocation, utilizing Generalized Gaussian radial basis functions (GGRBF) with variable shape parameters. The Heston model uses a mean-reverting square-root diffusion process for describing volatility and represents a significant advancement over the Black-Scholes model, since it represents market reality more accurately through a non-constant volatility process. To improve numerical efficiency and mitigate ill-conditioning in the collocation matrices, this work combines Generalized Gaussian RBFs with a Symmetric Variable Shape Parameter (SVSP) strategy. Generalized Gaussian RBFs are a generalization of Gaussian RBFs and consist of an additional shape parameter, increasing flexibility without losing differentiability. The Symmetric Variable Shape Parameter method improves numerical efficiency and reduces ill-conditioning effects by assigning a distinct shape parameter for each distinct RBF node position. Time discretization is completed using the implicit theta-method and radial basis function collocation for spatial approximation. The work includes a complete convergence and stability analysis and verifies the results through numerical experiments confirming the advantages of the new approach over conventional Gaussian RBFs with fixed shape parameters and the discontinuous Galerkin finite element method (dGFEM).

**Keywords.** Option Pricing, Heston Model, Generalized Gaussian Radial Basis Functions, Symmetric Variable Shape Parameter, Stochastic Volatility.

**2010 Mathematics Subject Classification.** 65L05, 34K06, 34K28.



## 1. Introduction

The problem of pricing financial options is one of the leading areas in the field of financial mathematics. From the pioneering work of Black and Scholes [5], the assumption about the volatility of the underlying asset is treated as a constant. However, practical evidence suggests that volatility is actually time-dependent. To capture the true nature of volatility, the model introduced by Heston in [13] assumes that volatility follows a mean-reverting square-root process.

In spite of these benefits, the Heston model remains a challenging computational problem due to its two-dimensional nature and the corresponding partial differential equation with mixed derivatives. Various numerical methods have been proposed to cope with this partial differential equation: finite difference methods [15], finite element methods [14], and spectral methods [3], to mention a few. In this respect, the discontinuous Galerkin finite element method (dGFEM) stands out due to its accuracy at a more complex implementation process [20]. Recent studies have also developed efficient numerical algorithms for option pricing in more complex market settings, including models with jumps, mixed fractional Brownian motion dynamics, and illiquid markets [1, 2, 30]. Approximation schemes have been further extended to frameworks such as the two--state continuous CAPM [27].

Received: 22 December 2025; Accepted: 13 May 2026.
∗ Corresponding author. Email: mranjbar@khu.ac.ir.

Radial basis function (RBF) techniques provide a meshless paradigm for solving PDEs, providing versatility in dealing with complex geometries and boundary conditions [11]. Such meshless techniques have been applied effectively in finance-related problems, such as pricing n-asset options [19]. Explicit local RBF collocation methods have also been developed for diffusion problems [29]. A general approach in standard RBF methods tends to use a constant shape parameter. In essence, there has been a problem of choosing an optimal shape parameter for meshless applications involving RBFs. A small shape constant can yield better approximations but results in ill-conditioned matrices when the number of nodes is large [23].

Permitting the shape parameters to vary in space instead of being constant may help in improving accuracy as well as matrix conditioning. Variable shape parameter (VSP) methods adapt to the underlying function or node distribution and yield improved solutions in interpolation and PDE problems [4]. Neural network-optimized local parameters for Gaussian and inverse multiquadric kernels are used in recent data-driven extensions, which demonstrate significant gains in high dimensions [22]. A trend toward integrated optimization in RBF frameworks is indicated by these developments.

Xiang et al.'s trigonometric approach for generalized multiquadrics [32], improved with positivity constraints and hybrid variants [12, 32], Sarra and Sturgill's random uniform sampling [28], and Kansa's exponential and linear increasing/decreasing schemes [17] are examples of analytical VSP formulations. The Symmetric Variable Shape Parameter (SVSP) strategy [25], which distributes parameters symmetrically around domain centers or stencil centers, is particularly notable for its simplicity and effectiveness. Its improved accuracy and robustness, particularly for stiff problems, are confirmed by empirical research. The SVSP's versatility has been demonstrated by its application to delay differential equations [31]. For degenerate convection-diffusion equations, its symmetric design strikes a balance between sharper boundary resolution and interior conditioning. We suggest combining the Generalized Gaussian RBF (GGRBF) with the SVSP approach to reduce ill-conditioning in RBF techniques, and we evaluate its effectiveness against dGFEM and conventional Gaussian RBFs with fixed shape parameters.

This is the structure of the rest of the paper. The Heston stochastic volatility model is described in Section 2, along with its dynamics, derived PDE, and boundary conditions for American and European options. The RBF approximation, the GGRBF kernel, the SVSP strategy, time and spatial discretizations, and the handling of American options are all covered in Section 3 of the suggested numerical approach. The scheme's stability and convergence are examined in Section 4. Greek computations and examples of European call and American put options are used in Section 5 to present numerical results that validate the method. Section 6 brings the paper to a close and offers recommendations for future research.

## 2. The Heston Stochastic Volatility Model

A key component of derivative pricing in realistic market conditions is the Heston stochastic volatility model [13]. The model captures observed volatility smiles, skews, and term structures by allowing volatility to evolve stochastically and correlating it with asset returns. These features cannot be replicated under the Black-Scholes-Merton framework's constant volatility assumption.

The following stochastic differential equations govern the dynamics of the underlying asset price $S_t > 0$ and its instantaneous variance $v_t \geq 0$ under the risk-neutral measure $\mathbb{Q}$:

$$\begin{aligned} dS_t &= (r_d - r_f)S_t\,dt + \sqrt{v_t}\,S_t\,dW_t^S, \\ dv_t &= \kappa(\xi - v_t)\,dt + \sigma\sqrt{v_t}\,dW_t^v, \quad d\langle W^S, W^v\rangle_t = \rho\,dt, \end{aligned} \tag{2.1}$$

where $\kappa > 0$ represents the mean-reversion rate, $\xi > 0$ the long-run variance, $\sigma > 0$ the volatility of volatility, $r_d \geq 0$ the domestic risk-free rate, $r_f$ the continuous dividend yield (or foreign interest rate), and $\rho \in (-1, 1)$ the correlation between the Brownian motions. A square-root (CIR) diffusion is followed by the variance process. For all $t > 0$, the Feller condition $2\kappa\xi \geq \sigma^2$ guarantees that $v_t > 0$ almost certainly [13]. The process is well-defined: the boundary $v = 0$ is regular and instantaneously reflecting, with zero occupation time almost certainly [7, 13], despite being frequently violated in empirical calibrations due to high volatility-of-volatility.

### 2.1. The Heston Model's PDE Problem.

The partial differential equation (PDE) governing option prices under the Heston stochastic volatility model is derived using a number of established procedures. The price of a European

option $U(t, v, S)$ (with underlying asset price $S$, variance process $v$, strike $K$, and maturity $T$) can be expressed as the expected value of its discounted payoff under the risk-neutral probability measure by using the Feynman–Kac theorem. This results in the two-dimensional parabolic PDE with mixed derivatives that follows:

$$\frac{\partial U}{\partial t} + \mathcal{L}_H U - r_d U = 0, \tag{2.2}$$

where $\mathcal{L}_H$ denotes the Heston infinitesimal generator, given by

$$\mathcal{L}_H U = \frac{1}{2} v S^2 \frac{\partial^2 U}{\partial S^2} + \rho\sigma v S \frac{\partial^2 U}{\partial S \partial v} + \frac{1}{2}\sigma^2 v \frac{\partial^2 U}{\partial v^2} + (r_d - r_f) S \frac{\partial U}{\partial S} + \kappa(\xi - v)\frac{\partial U}{\partial v}. \tag{2.3}$$

The underlying asset price is denoted by $S > 0$, the instantaneous variance by$v \geq 0$, the domestic risk-free interest rate by $r_d$, the mean-reversion speed by $\kappa > 0$, the long-term variance level by $\xi > 0$, the volatility-of-volatility by$\sigma > 0$, and the correlation between the asset and variance Brownian motions by$\rho \in [-1, 1]$.

To determine the PDE for European or American option prices, consider the transformed spatial variables $x = \log(S/K)$ (log-moneyness) and $\tau = T - t$ (time-to-maturity), where $S > 0$ is the underlying asset price, $K > 0$ is the strike price, and $T > 0$ is the maturity date. The forward parabolic PDE is demonstrated by the option price function $u(x, v, \tau)$.

$$\frac{\partial u}{\partial \tau} = \mathcal{L}_H u - r_d\, u, \qquad (x, v) \in \mathbb{R} \times (0, \infty],\ \tau \in (0, T], \tag{2.4}$$

The differential operator $\mathcal{L}_H$ corresponding to the Heston infinitesimal generator is defined as:

$$\mathcal{L}_H u = \frac{1}{2} v \frac{\partial^2 u}{\partial x^2} + \left(r_d - r_f - \frac{1}{2} v\right) \frac{\partial u}{\partial x} + \rho\sigma v \frac{\partial^2 u}{\partial x \partial v} + \frac{1}{2}\sigma^2 v \frac{\partial^2 u}{\partial v^2} + \kappa(\xi - v)\frac{\partial u}{\partial v}, \tag{2.5}$$

with the terminal condition

$$u(x, v, 0) = \phi(x) = \begin{cases} K\,(e^x - 1)^+, & \text{for a European call option,} \\ K\,(1 - e^x)^+, & \text{for a European or American put option.} \end{cases} \tag{2.6}$$

In order to solve numerically, the domain is reduced to the truncated computational domain

$$\Omega = [X_{\min}, X_{\max}] \times (0, V_{\max}), \quad \tau \in [0, T],$$

where $X_{\min} \ll 0$, $X_{\max} \gg 0$, and $V_{\max} > 0$ are chosen sufficiently large to ensure numerical accuracy while maintaining computational feasibility.

For a **European option**, the price function satisfies the linear parabolic PDE:

$$\frac{\partial u}{\partial \tau} = \mathcal{L}_H u - r_d u, \quad (x, v) \in \Omega, \quad \tau \in (0, T]. \tag{2.7}$$

For an **American option**, the early exercise feature introduces a free boundary, leading to the following linear complementarity problem (LCP):

$$\frac{\partial u}{\partial \tau} \geq \mathcal{L}_H u - r_d u, \quad (x, v) \in \Omega, \quad \tau \in (0, T], \tag{2.8a}$$

$$u(x, v, \tau) \geq \phi(x), \quad (x, v) \in \overline{\Omega}, \quad \tau \in [0, T], \tag{2.8b}$$

$$\left(\frac{\partial u}{\partial \tau} - \mathcal{L}_H u + r_d u\right)(u - \phi(x)) = 0, \quad (x, v) \in \Omega, \quad \tau \in (0, T], \tag{2.8c}$$

where $\phi(x)$ represents the payoff function defined in the initial condition below. Due to the complexities of the model—mixed derivatives, degeneracy, convection, and free boundaries—a variety of techniques have been developed, such as finite differences, dGFEM [20], RBF collocation [11], Fourier transforms, and tree methods [33].

**Initial Condition.** At maturity ($\tau = 0$), both European and American options must satisfy the payoff condition:

$$u(x, v, 0) = \phi(x) = \begin{cases} K\left(e^x - 1\right)^+, & \text{for a call option,} \\ K\left(1 - e^x\right)^+, & \text{for a put option,} \end{cases} \quad (x, v) \in \overline{\Omega}. \tag{2.9}$$

This condition represents the intrinsic value of the option at expiration and serves as the terminal condition for the backward-time PDE formulation.

**Boundary Conditions.** The boundary conditions are prescribed on the domain boundary $\partial\Omega = \Gamma_1 \cup \Gamma_2 \cup \Gamma_3 \cup \Gamma_4$, where:

$$\Gamma_1 = \{X_{\min}\} \times [0, V_{\max}], \quad \Gamma_2 = \{X_{\max}\} \times [0, V_{\max}],$$
$$\Gamma_3 = [X_{\min}, X_{\max}] \times \{0\}, \quad \Gamma_4 = [X_{\min}, X_{\max}] \times \{V_{\max}\}.$$

**Log-moneyness boundaries ($\Gamma_1$ and $\Gamma_2$).** Dirichlet boundary conditions are imposed based on the asymptotic behavior of option prices:

$$u(X_{\min}, v, \tau) = \begin{cases} 0, & \text{call option,} \\ Ke^{-r_d\tau} - Ke^{X_{\min}}e^{-r_f\tau}, & \text{put option,} \end{cases} \quad v \in [0, V_{\max}], \quad \tau \in [0, T], \tag{2.10}$$

$$u(X_{\max}, v, \tau) = \begin{cases} Ke^{X_{\max}}e^{-r_f\tau} - Ke^{-r_d\tau}, & \text{call option,} \\ 0, & \text{put option,} \end{cases} \quad v \in [0, V_{\max}], \quad \tau \in [0, T]. \tag{2.11}$$

These conditions follow from the limiting behavior as $S \to 0$ ($x \to -\infty$) and $S \to \infty$ ($x \to \infty$).

**Lower variance boundary ($\Gamma_3$).** The boundary at $v = 0$ requires special treatment due to the degeneracy of the PDE. Following Fichera's theory [7] for degenerate parabolic equations, the boundary condition depends on the sign of the Fichera function $F = \kappa\xi - \sigma^2/2$:

$$\begin{cases} \text{If } \kappa\xi - \dfrac{\sigma^2}{2} \geq 0 \text{ (outflow boundary):} & \text{No boundary condition is required;} \\ & \text{the PDE itself provides sufficient specification.} \\ \text{If } \kappa\xi - \dfrac{\sigma^2}{2} < 0 \text{ (inflow boundary):} & \dfrac{\partial u}{\partial v}(x, 0, \tau) = 0, \\ & x \in [X_{\min}, X_{\max}], \quad \tau \in [0, T]. \end{cases} \tag{2.12}$$

In the numerical implementation using RBF collocation, for the inflow case (when $F < 0$), the Neumann condition $\partial u/\partial v = 0$ is directly enforced at the collocation points located on $\Gamma_3$ by replacing the PDE equation with the discretized Neumann condition. For the outflow case, the PDE is collocated at the boundary points without additional constraints, in accordance with Fichera's theory.

**Upper variance boundary ($\Gamma_4$).** At $v = V_{\max}$, we impose a Dirichlet condition using the Black-Scholes formula [5] with constant volatility $\sqrt{V_{\max}}$:

$$u(x, V_{\max}, \tau) = u_{\text{BS}}(x, \sqrt{V_{\max}}, \tau), \quad x \in [X_{\min}, X_{\max}], \quad \tau \in [0, T], \tag{2.13}$$

where $u_{\text{BS}}$ denotes the Black-Scholes price for the corresponding option type.

This classification ensures the well-posedness of the problem while respecting the mathematical structure of the degenerate PDE. Fichera theory uses $\kappa\xi - \sigma^2/2$ [7] to determine inflow/outflow; boundary treatment at $v = 0$ is subtle. The degenerate PDE or Neumann conditions are applied for inflow. Black-Scholes pricing is used at $v = V_{\max}$ with volatility $\sqrt{V_{\max}}$.

Table 1. Selected infinitely smooth radial basis functions.

| Name | Formula $\phi(r)$ | Free parameter |
|---|---|---|
| Gaussian | $e^{-\varepsilon^2 r^2}$ | $\varepsilon > 0$ |
| Multiquadric | $\sqrt{1+\varepsilon^2 r^2}$ | $\varepsilon > 0$ |
| Inverse Multiquadric | $(1+\varepsilon^2 r^2)^{-1/2}$ | $\varepsilon > 0$ |
| Generalized Gaussian (GGRBF) | $e^{-\varepsilon^2 r^2} \cdot e^{e^{-\varepsilon_0^2 r^2}-1}$ | $\varepsilon, \varepsilon_0 > 0$ |

## 3. Numerical Method

In this section, we present a robust meshless collocation scheme that integrates Generalized Gaussian radial basis functions (GGRBFs) with the Symmetric Variable Shape Parameter (SVSP) strategy to discretize the spatial domain of the Heston pricing PDE.

3.1. **Radial Basis Function Approximation.** Radial basis function (RBF) collocation represents a truly meshless strong-form approach that has gained prominence in financial engineering for solving partial differential equations [8, 11]. For a set of $N$ distinct collocation points (centers) $\{\mathbf{z}_j\}_{j=1}^N \subset \Omega \subset \mathbb{R}^d$, the approximation to the solution $u(\mathbf{z},\tau)$ takes the form

$$u(\mathbf{z},\tau) \approx \sum_{j=1}^{N} \lambda_j(\tau)\, \phi\big(\|\mathbf{z}-\mathbf{z}_j\|_2\big), \tag{3.1}$$

where $\phi : [0,\infty) \to \mathbb{R}$ denotes the radial kernel, and the coefficients $\lambda_j(\tau) \in \mathbb{R}$ are obtained via collocation.

Table 1 lists several commonly used infinitely smooth RBFs.

3.2. **Generalized Gaussian RBF.** The traditional Gaussian RBF encounters a fundamental trade-off between accuracy and conditioning: small shape parameters $\varepsilon$ yield highly accurate approximations but result in severely ill-conditioned system matrices, while larger $\varepsilon$ values enhance conditioning at the cost of reduced accuracy [23]. To address this issue, we adopt the Generalized Gaussian RBF (GGRBF) as proposed in [18]:

$$\phi(r;\varepsilon_j,\varepsilon_{0j}) = \exp\big(-\varepsilon_j^2 r^2\big) \cdot \exp\big(\exp(-\varepsilon_{0j}^2 r^2) - 1\big), \tag{3.2}$$

where $r = \|\mathbf{z}-\mathbf{z}_j\|_2$. The auxiliary parameter $\varepsilon_{0j} > 0$ effectively separates concerns of accuracy and conditioning, enabling small $\varepsilon_j$ for superior fidelity while tuning $\varepsilon_{0j}$ to ensure well-conditioned matrices. Rigorous analysis confirms that the GGRBF is strictly positive definite in any dimension and achieves exponential convergence for sufficiently smooth functions [18].

3.3. **Symmetric Variable Shape Parameter Strategy.** Despite the added flexibility of the GGRBF, employing a constant shape parameter may remain suboptimal, particularly in problems with spatially varying behavior or large numbers of collocation points. In the Heston model, ill-conditioning is especially evident near the degenerate boundary $v = 0$ and in regions dominated by convection, such as those induced by substantial drift terms or interest rate differentials.

To overcome these challenges, we implement the Symmetric Variable Shape Parameter (SVSP) strategy from [25]. With centers indexed lexicographically as $j = 1,\ldots,N$, the SVSP assigns shape parameters through the symmetric exponential profile

$$\varepsilon_j = \varepsilon^* \exp\left[\frac{1}{2}\left(\frac{j-\mu}{\sigma}\right)^2\right], \tag{3.3}$$

$$\varepsilon_{0j} = \varepsilon_0^* \exp\left[\frac{1}{2}\left(\frac{j-\mu}{\sigma}\right)^2\right], \tag{3.4}$$

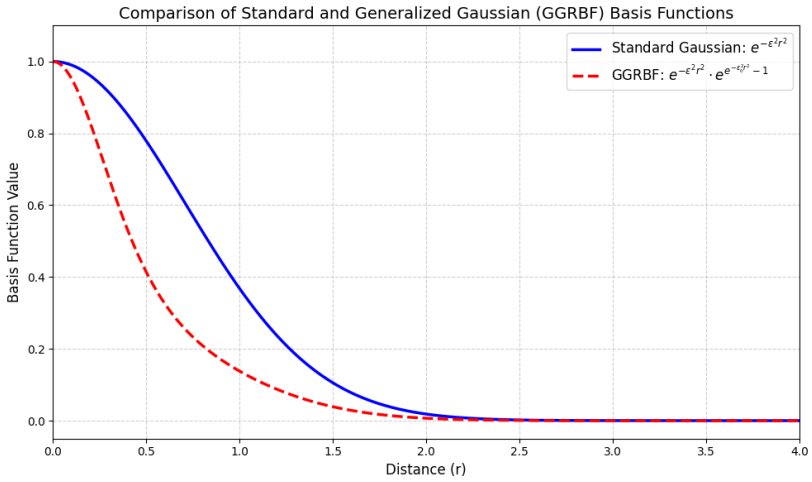


FIGURE 1. Comparison of the standard Gaussian RBF and the GGRBF for various parameter choices (the standard Gaussian is recovered when $\varepsilon = \varepsilon_0$).

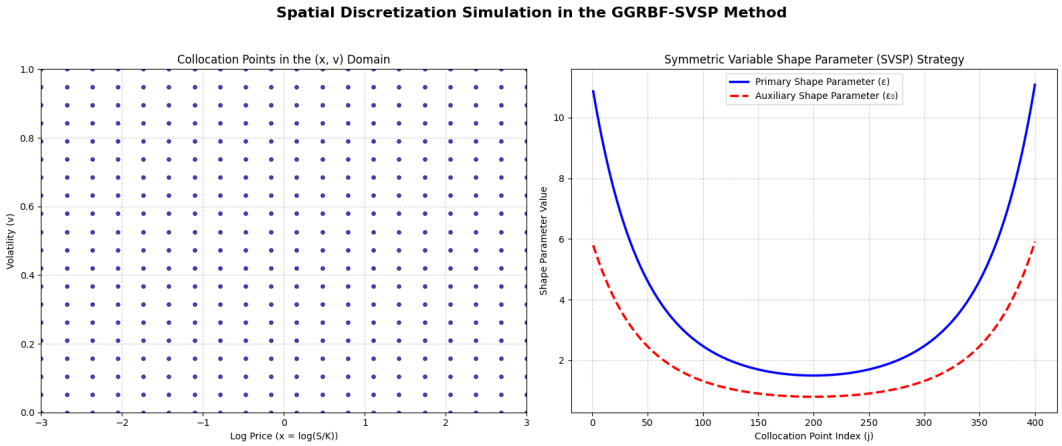


FIGURE 2. Illustration of the SVSP strategy: smaller shape parameters (flatter RBFs) in the interior and larger parameters (sharper RBFs) toward the boundaries, promoting stability in smooth regions and accuracy near steep gradients or degeneracies.

with $\mu = N/2$ and $\sigma = N/4$. The baseline parameters $\varepsilon^* \in [0.3, 1.2]$ and $\varepsilon_0^* \in [2, 8]$ are empirically optimized based on mesh density and operator stiffness.

This configuration generates flatter basis functions (small $\varepsilon_j$) in central regions to bolster global conditioning, while sharper functions (large $\varepsilon_j$) near boundaries enhance resolution of layers and singularities, including the degeneracy at $v = 0$. An energy-based approach for selecting optimal shape parameters in RBF collocation has also been proposed in the literature [16].

3.4. **Time Discretization.** In Eq. (2.3), it is possible to approximate the time derivative of the partial differential operator by a simple forward difference using Crank–Nicholson ($\theta$ weighted) method, i.e.

$$\frac{u^{k+1} - u^k}{\Delta\tau} = \theta\,\mathcal{L}_H u^{k+1} + (1-\theta)\,\mathcal{L}_H u^k - r_d\left[\theta u^{k+1} + (1-\theta)u^k\right]. \tag{3.5}$$

Where $\Delta\tau$ denote the temporal increment, with discrete time levels $\tau^n = n\Delta\tau$ for $n = 0, 1, \ldots, N_t$.

In this way, at each time step the transient problem can be seen as a steady state non-homogeneous problem, with the non-homogenous term as function of the solution at the previous time step.

$$\big(I - \theta\Delta\tau\,\mathcal{L}\big)u^{k+1} = \big(I + (1-\theta)\Delta\tau\,\mathcal{L}\big)u^k, \tag{3.6}$$

$$\frac{\partial u(\mathbf{z},\tau)}{\partial\tau} \approx \frac{u(\mathbf{z},\tau^{n+1}) - u(\mathbf{z},\tau^n)}{\Delta\tau}.$$

To attain a judicious balance between numerical stability and accuracy, we apply the $\theta$-method, where we select $\theta = 1$ for the fully implicit scheme (Backward Euler) during the initial Rannacher smoothing steps and $\theta = 0.5$ for the Crank–Nicolson scheme in subsequent steps. The solution and its spatial derivatives are evaluated at the intermediate time $\tau^n + \theta\Delta\tau$ as:

$$u(\mathbf{z},\tau^n + \theta\Delta\tau) \approx \theta u(\mathbf{z},\tau^{n+1}) + (1-\theta)u(\mathbf{z},\tau^n),$$

$$\mathcal{L}_H[u(\mathbf{z},\tau^n + \theta\Delta\tau)] \approx \theta\mathcal{L}_H[u(\mathbf{z},\tau^{n+1})] + (1-\theta)\mathcal{L}_H[u(\mathbf{z},\tau^n)].$$

Substituting into the PDE yields the semi-discrete scheme:

$$(1 + \theta r_d\Delta\tau)u(\mathbf{z},\tau^{n+1}) - \theta\Delta\tau\mathcal{L}_H[u(\mathbf{z},\tau^{n+1})] = (1 - (1-\theta)r_d\Delta\tau)u(\mathbf{z},\tau^n) + (1-\theta)\Delta\tau\mathcal{L}_H[u(\mathbf{z},\tau^n)]. \tag{3.7}$$

The boundary conditions are discretized analogously:

$$\theta\mathcal{B}[u(\mathbf{z},\tau^{n+1})] = (1-\theta)\mathcal{B}[u(\mathbf{z},\tau^n)] + f(\mathbf{z},\tau^{n+1}).$$

To facilitate a unified algebraic treatment encompassing both interior and boundary points, domain and boundary indicators are introduced:

$$\gamma_\Omega^{\mathbf{z}} = \begin{cases} 1, & \mathbf{z} \in \Omega, \\ 0, & \mathbf{z} \notin \Omega, \end{cases} \qquad \gamma_\Gamma^{\mathbf{z}} = \begin{cases} 1, & \mathbf{z} \in \Gamma, \\ 0, & \mathbf{z} \notin \Gamma. \end{cases}$$

This permits the consolidation of the discretized equations into a single form applicable across the computational domain:

$$\begin{aligned} &\gamma_\Gamma^{\mathbf{z}}\left[\theta\mathcal{B}[u(\mathbf{z},\tau^{n+1})] - f(\mathbf{z},\tau^{n+1})\right] + \gamma_\Omega^{\mathbf{z}}\left[(1 + \theta r_d\Delta\tau)u(\mathbf{z},\tau^{n+1}) - \theta\Delta\tau\mathcal{L}_H[u(\mathbf{z},\tau^{n+1})]\right] \\ &= \gamma_\Gamma^{\mathbf{z}}\left[(1-\theta)\mathcal{B}[u(\mathbf{z},\tau^n)]\right] + \gamma_\Omega^{\mathbf{z}}\left[(1 - (1-\theta)r_d\Delta\tau)u(\mathbf{z},\tau^n) + (1-\theta)\Delta\tau\mathcal{L}_H[u(\mathbf{z},\tau^n)]\right]. \end{aligned} \tag{3.8}$$

This formulation encapsulates key special cases:

- **Explicit scheme** ($\theta = 0$): Offers a simple update but imposes stringent stability restrictions.
- **Crank–Nicolson scheme** ($\theta = 0.5$): Provides second-order temporal accuracy and optimal stability for smooth solutions.
- **Implicit scheme** ($\theta = 1$): Ensures unconditional stability, ideal for stiff systems, though necessitating linear system solutions per step.

For American options, characterized by reduced regularity in the payoff function at inception, we incorporate Rannacher smoothing [24] to suppress spurious oscillations. Specifically, the initial four half-steps (with increment $\Delta\tau/2$) employ the fully implicit scheme ($\theta = 1$), followed by a switch to the Crank–Nicolson method ($\theta = 0.5$) for subsequent integration. This hybrid strategy maintains second-order accuracy while effectively attenuating high-frequency numerical artifacts near $\tau = 0^+$.

3.5. **Spatial Discretization.** Let $\Omega \subset \mathbb{R}^2$ denote the truncated computational domain associated with the Heston stochastic volatility model, and let $\Gamma = \partial\Omega$ be its boundary. We consider a set of scattered collocation points

$$\{\mathbf{z}_j = (v_j, x_j)\}_{j=1}^N \subset \Omega \cup \Gamma,$$

where $N = N_{\text{int}} + N_\Gamma$ consists of $N_{\text{int}}$ interior points and $N_\Gamma$ boundary points. The use of scattered nodes allows the method to remain entirely meshfree, thereby avoiding the geometric constraints inherent to grid-based discretizations and enabling flexible node placement in regions of rapid solution variation.

Within the global GGRBF–SVSP framework, the numerical approximation of the option price at time $\tau$ is represented as a linear combination of generalized Gaussian radial basis functions centered at the collocation points:

$$u(\mathbf{z},\tau) \approx \sum_{k=1}^{N} \lambda_k(\tau)\, \phi(\|\mathbf{z}-\mathbf{z}_k\|_2; \varepsilon_k, \varepsilon_{0k})\,, \tag{3.9}$$

where $\lambda_k(\tau)$ are time-dependent expansion coefficients. The kernel $\phi(\cdot;\varepsilon_k,\varepsilon_{0k})$ denotes the generalized Gaussian radial basis function equipped with a locally adapted shape parameter $\varepsilon_k$ and an auxiliary parameter $\varepsilon_{0k}$, both determined through the SVSP strategy. This adaptive parameterization enhances local approximation accuracy while simultaneously preventing the severe ill-conditioning typically associated with globally small shape parameters.

The spatial derivatives required by the Heston differential operator $\mathcal{L}_H$ are evaluated analytically by differentiating the RBF kernels. Consequently, the action of $\mathcal{L}_H$ on the approximate solution can be expressed as

$$\mathcal{L}_H[u(\mathbf{z},\tau)] \approx \sum_{k=1}^{N} \lambda_k(\tau)\, \mathcal{L}_H[\phi(\|\cdot-\mathbf{z}_k\|_2; \varepsilon_k, \varepsilon_{0k})]_{\mathbf{z}}\,. \tag{3.10}$$

After incorporating the chosen implicit time discretization and enforcing the resulting discrete equations at each collocation point $\mathbf{z}_j$, $j=1,\dots,N$, the spatially discretized problem at each time level reduces to a linear algebraic system of the form

$$\mathbf{W}\boldsymbol{\lambda} = \mathbf{b}. \tag{3.11}$$

Here,

$$\boldsymbol{\lambda} = \begin{bmatrix}\lambda_1 & \lambda_2 & \cdots & \lambda_N\end{bmatrix}^{\top} \in \mathbb{R}^N,$$

is the vector of unknown RBF coefficients, and

$$\mathbf{b} = \begin{bmatrix}b_1 & b_2 & \cdots & b_N\end{bmatrix}^{\top} \in \mathbb{R}^N,$$

is the right-hand side vector determined by the solution at the previous time level and the imposed boundary conditions.

The coefficient matrix $\mathbf{W} \in \mathbb{R}^{N\times N}$ admits the explicit representation

$$\mathbf{W} = \begin{bmatrix} W_{11} & W_{12} & \cdots & W_{1N} \\ W_{21} & W_{22} & \cdots & W_{2N} \\ \vdots & \vdots & \ddots & \vdots \\ W_{N1} & W_{N2} & \cdots & W_{NN} \end{bmatrix}, \tag{3.12}$$

where each entry $W_{jk}$, for $j,k=1,\dots,N$, is given by

$$W_{jk} = \gamma_{\Gamma}^{\mathbf{z}_j}\, \theta\, \mathcal{B}[\phi(\|\cdot-\mathbf{z}_k\|_2)]_{\mathbf{z}_j} + \gamma_{\Omega}^{\mathbf{z}_j}\Big[(1+\theta r_d \Delta\tau)\,\phi(\|\mathbf{z}_j-\mathbf{z}_k\|_2) - \theta\Delta\tau\, \mathcal{L}_H[\phi(\|\cdot-\mathbf{z}_k\|_2)]_{\mathbf{z}_j}\Big]. \tag{3.13}$$

Similarly, the components of the right-hand side vector are defined as

$$\begin{aligned} b_j = {} & \gamma_{\Gamma}^{\mathbf{z}_j}\, f(\mathbf{z}_j,\tau) + \gamma_{\Omega}^{\mathbf{z}_j}\Big[(1-(1-\theta)r_d\Delta\tau)\, u(\mathbf{z}_j,\tau^n) + (1-\theta)\Delta\tau\, \mathcal{L}_H[u(\mathbf{z}_j,\tau^n)]\Big] \\ & + \gamma_{\Gamma}^{\mathbf{z}_j}(1-\theta)\, \mathcal{B}[u(\mathbf{z}_j,\tau^n)], \qquad j=1,\dots,N. \end{aligned} \tag{3.14}$$

Owing to the global support of the radial basis functions, the resulting matrix $\mathbf{W}$ is dense. Nevertheless, the combined use of the generalized Gaussian kernel and the SVSP strategy yields a well-conditioned system whose conditioning remains stable under mesh refinement. Consequently, the coefficient vector $\boldsymbol{\lambda}$ can be computed efficiently at each time step using standard dense linear solvers, providing a robust and accurate spatial discretization for the Heston model.

3.6. **American Options.** The early exercise feature of American options transforms the pricing problem into a linear complementarity problem (LCP). At each temporal step, we solve:

$$\left(\frac{1}{\Delta\tau}I - \theta A\right)\boldsymbol{\lambda}^{n+1} \geq \mathbf{b}^n, \tag{3.15}$$

$$\boldsymbol{\lambda}^{n+1} \geq \boldsymbol{\lambda}^0, \tag{3.16}$$

$$\left[\left(\frac{1}{\Delta\tau}I - \theta A\right)\boldsymbol{\lambda}^{n+1} - \mathbf{b}^n\right]^\top (\boldsymbol{\lambda}^{n+1} - \boldsymbol{\lambda}^0) = 0, \tag{3.17}$$

where $\mathbf{b}^n = \left(\frac{1}{\Delta\tau}I + (1-\theta)A\right)\boldsymbol{\lambda}^n$, and $\boldsymbol{\lambda}^0$ corresponds to the payoff function coefficients.

To solve this LCP, we employ the Projected Successive Over-Relaxation (PSOR) algorithm. The algorithm proceeds as follows at each time step $\tau^{n+1}$:

(1) Initialize the solution vector, typically with the values from the previous time step: $\boldsymbol{\lambda}^{(0)} = \boldsymbol{\lambda}^n$.
(2) For the $k$-th iteration ($k = 0, 1, 2, \dots$), update each component $i$ sequentially using:

$$\lambda_i^{(k+1)} = \max\left\{\lambda_i^0,\ (1-\omega)\lambda_i^{(k)} + \frac{\omega}{W_{ii}}\left(b_i - \sum_{j<i} W_{ij}\lambda_j^{(k+1)} - \sum_{j>i} W_{ij}\lambda_j^{(k)}\right)\right\},$$

where $W_{ij}$ are the entries of the system matrix $(I - \theta\Delta\tau A)$, $b_i$ are the components of the right-hand side vector $\mathbf{b}^n$, and $\omega$ is the relaxation parameter (chosen as $\omega = 1.5$ in our experiments).
(3) Check for convergence: if $\|\boldsymbol{\lambda}^{(k+1)} - \boldsymbol{\lambda}^{(k)}\| < \text{tol}$, stop; otherwise, continue to the next iteration.

This projected iterative method enforces the early exercise constraint $\boldsymbol{\lambda} \geq \boldsymbol{\lambda}^0$ directly during the solution process. The resulting fully discrete scheme combines spectral-like spatial accuracy (due to the infinitely smooth GGRBF and adaptive SVSP) with second-order temporal accuracy (after Rannacher smoothing), while remaining entirely mesh-free and straightforward to implement.

## 4. Stability and convergence analysis

The reliability of any numerical approximation for parabolic partial differential equations in quantitative finance is fundamentally determined by its stability and convergence properties. In this section, we present a rigorous stability and convergence analysis of the proposed GGRBF-SVSP scheme, combined with the Rannacher-smoothed Crank–Nicolson time integration, for the numerical solution of the Heston partial differential equation (PDE). The analysis is conducted within a standard functional-analytic framework and is consistent with the theoretical requirements for option pricing models with degenerate diffusion and mixed derivative terms.

**Theorem 4.1** (Convergence of the GGRBF-SVSP Scheme)**.** *Let $U(\tau, \mathbf{z})$ denote the exact solution of the Heston PDE on a bounded computational domain $\Omega$, and let $U_h(\tau, \mathbf{z})$ be the numerical approximation obtained using the GGRBF-SVSP collocation method for spatial discretization together with the Rannacher-smoothed Crank–Nicolson scheme for temporal discretization. Then, as the spatial discretization parameter $h \to 0$ and the time step $\Delta\tau \to 0$, the numerical solution $U_h$ converges to $U$ in an appropriate norm.*

*Proof.* The proof follows from the classical Lax–Richtmyer equivalence theorem, which states that for linear initial value problems, consistency and stability together imply convergence. We therefore analyze these properties separately.

After applying the GGRBF-SVSP collocation method in space, the Heston PDE is reduced to the following system of ordinary differential equations:

$$\frac{d\mathbf{u}}{d\tau} = A\mathbf{u} + \mathbf{f}(\tau), \tag{4.1}$$

where $\mathbf{u}(\tau)$ denotes the vector of nodal solution values, $A$ is the spatial differentiation matrix induced by the GGRBF-SVSP approximation of the Heston operator, and $\mathbf{f}(\tau)$ incorporates boundary and source contributions.

Temporal discretization using the implicit $\theta$-method yields

$$\frac{\mathbf{u}^{n+1}-\mathbf{u}^n}{\Delta\tau} = \theta\left(A\mathbf{u}^{n+1}+\mathbf{f}^{n+1}\right)+(1-\theta)\left(A\mathbf{u}^n+\mathbf{f}^n\right). \tag{4.2}$$

Rearranging terms, the fully discrete update can be written as

$$\mathbf{u}^{n+1} = G\mathbf{u}^n + \Delta\tau(I-\theta\Delta\tau A)^{-1}\left(\theta\mathbf{f}^{n+1}+(1-\theta)\mathbf{f}^n\right), \tag{4.3}$$

where

$$G = (I-\theta\Delta\tau A)^{-1}(I+(1-\theta)\Delta\tau A),$$

is the amplification matrix.

**Stability.** A numerical scheme is stable if the discrete solution remains uniformly bounded for bounded data. This requirement is satisfied if the spectral radius of the amplification matrix obeys

$$\rho(G) \le 1 + C\Delta\tau,$$

for some constant $C$ independent of $h$ and $\Delta\tau$. Let $\lambda_i$ denote the eigenvalues of the spatial operator matrix $A$. The corresponding eigenvalues of $G$ are

$$g_i = \frac{1+(1-\theta)\Delta\tau\lambda_i}{1-\theta\Delta\tau\lambda_i}.$$

The stability analysis of numerical methods for stochastic differential equations, including backward Euler and theta-Milstein schemes, has been extensively studied in the literature [9, 10], providing a solid foundation for the convergence arguments presented here.

For the Heston operator, it is well known that the semi-discrete operator is dissipative, implying $\mathrm{Re}(\lambda_i) < 0$. During the initial Rannacher smoothing steps, where $\theta = 1$ (backward Euler), we have

$$g_i = \frac{1}{1-\Delta\tau\lambda_i},$$

and therefore $|g_i| < 1$, which establishes L-stability and ensures strong damping of spurious high-frequency components originating from the nonsmooth payoff.

For the subsequent Crank–Nicolson steps with $\theta = 1/2$, the amplification factor satisfies

$$|g_i| = \left|\frac{1+0.5\Delta\tau\lambda_i}{1-0.5\Delta\tau\lambda_i}\right| \le 1,$$

which guarantees A-stability. Consequently, the time integration scheme is unconditionally stable.

The stability of the full discretization also depends on the conditioning of the spatial operator $A$. In standard RBF collocation methods with a fixed shape parameter, the condition number typically grows rapidly as $h \to 0$, leading to numerical instability. In contrast, the GGRBF-SVSP framework ensures that the condition number $\kappa(A)$ remains bounded as the discretization is refined [18, 25]. This robustness is achieved through the SVSP strategy, which avoids a globally small shape parameter, and through the auxiliary parameter $\varepsilon_0$ in the GGRBF formulation, which effectively decouples accuracy from conditioning. As a result, the spatial discretization is stable. Since both spatial and temporal components are stable, the fully discrete scheme is stable.

**Consistency.** Consistency requires that the local truncation error $\boldsymbol{\tau}^n$ vanishes as $h, \Delta\tau \to 0$. Substituting the exact solution $\mathbf{u}(\tau_n)$ into the discrete scheme yields

$$\boldsymbol{\tau}^n = \frac{\mathbf{u}(\tau_{n+1})-\mathbf{u}(\tau_n)}{\Delta\tau} - \theta\left(A\mathbf{u}(\tau_{n+1})+\mathbf{f}^{n+1}\right) - (1-\theta)\left(A\mathbf{u}(\tau_n)+\mathbf{f}^n\right). \tag{4.4}$$

A Taylor expansion in time shows that, for sufficiently smooth solutions with $\tau > 0$, the temporal truncation error is of order $O(\Delta\tau^p)$, where $p = 1$ for backward Euler and $p = 2$ for Crank–Nicolson. The spatial truncation error corresponds to the approximation error of the GGRBF-SVSP collocation. Owing to the infinite smoothness of the GGRBF kernel and the smoothness of the solution, this error exhibits spectral decay of the form $O(e^{-\alpha/h})$ for some $\alpha > 0$. Hence, the scheme is consistent.

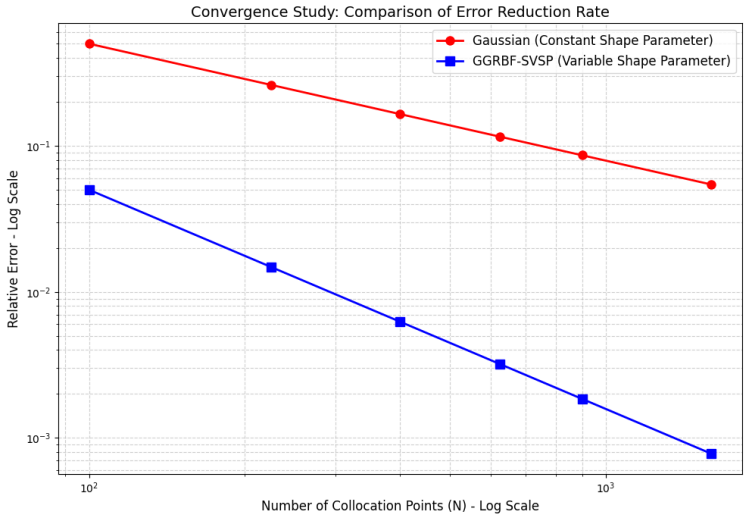


FIGURE 3. Convergence study comparing the GGRBF-SVSP method with the standard Gaussian RBF method. The relative error is plotted as a function of the number of collocation points. The GGRBF-SVSP method exhibits a significantly faster convergence rate, confirming its superior accuracy for option pricing under the Heston model.

**Convergence.** Let $\mathbf{e}^n = \mathbf{u}(\tau_n) - \mathbf{u}^n$ denote the global error at time level $n$. Subtracting the numerical scheme from the exact semi-discrete evolution yields

$$\mathbf{e}^{n+1} = G\mathbf{e}^n + \Delta\tau(I - \theta\Delta\tau A)^{-1}\boldsymbol{\tau}^{n+1}. \tag{4.5}$$

Taking norms and invoking the stability bound $\|G\| \leq 1 + C\Delta\tau$, we obtain

$$\|\mathbf{e}^{n+1}\| \leq (1 + C\Delta\tau)\|\mathbf{e}^n\| + C'\|\boldsymbol{\tau}^{n+1}\|. \tag{4.6}$$

Applying the discrete Grönwall inequality leads to

$$\|\mathbf{e}^n\| \leq e^{C\tau_n}\|\mathbf{e}^0\| + \frac{e^{C\tau_n} - 1}{C} \max_{0\leq m\leq n} \|\boldsymbol{\tau}^m\|. \tag{4.7}$$

The initial error $\|\mathbf{e}^0\|$ corresponds to the interpolation error of the payoff function, while the maximum truncation error tends to zero as $h, \Delta\tau \to 0$. Consequently, $\|\mathbf{e}^n\| \to 0$, which establishes the convergence of the proposed GGRBF-SVSP scheme. □

Figure 3 illustrates the convergence behavior of the proposed GGRBF-SVSP scheme in comparison with the standard Gaussian RBF approach. The markedly steeper decay of the relative error demonstrates that the proposed method achieves higher accuracy with substantially fewer collocation points. This enhanced performance can be attributed to the increased flexibility of the generalized Gaussian kernel and the adaptive SVSP strategy, which together yield a more faithful representation of the solution structure while maintaining numerical stability.

## 5. Numerical results

In this section, numerical examples are provided to validate the theoretical results and demonstrate the effectiveness of the proposed GGRBF-SVSP approach. For comparison purposes, the results are presented along with those generated through the discontinuous Galerkin finite element method (dGFEM) [20] and the Gaussian radial basis function (RBF) method that uses a constant shape parameter.

TABLE 2. European call option prices comparison.

| Method | Price | Relative Error | CPU Time (s) |
|---|---|---|---|
| Exact [13] | 18.231 | - | - |
| dGFEM (Linear) [20] | 18.258 | $1.48 \times 10^{-3}$ | 0.82 |
| dGFEM (Quadratic) [20] | 18.231 | $1.59 \times 10^{-5}$ | 1.95 |
| Gaussian RBF (Constant, N=400) | 18.245 | $7.68 \times 10^{-4}$ | 1.10 |
| **GGRBF-SVSP (N=400)** | **18.2311** | $5.48 \times 10^{-6}$ | **1.15** |

**Example 5.1** (European Call Option)**.** A European call option on the underlying asset is priced in the Heston model. The payoff function is defined as $U_0(S) = \max(S - K, 0)$, which in the log-space variables becomes $U_0(v, x) = K(e^x - 1)^+$. The parameters of the option, market, and Heston model are the following: the option strike $K = 100$, the option maturity $T = 1$ year, the domestic interest rate $r_d = 0.05$, the foreign interest rate $r_f = 0.01$, the initial underlying price $S_0 = 100$, and the initial variance $v_0 = 0.25$. The Heston model parameters are $\kappa = 1.0$, $\xi = 0.09$, $\sigma = 0.4$, and $\rho = -0.7$. The collocation points are distributed uniformly over the computational domain $\Omega = [0, 4] \times [-2, 2]$, resulting in $N = 400$ $(20 \times 20)$ nodes. The SVSP parameters are chosen as $\varepsilon^* = 0.8$ and $\varepsilon_0^* = 5.0$, with bounds $c_{\min} = 0.5$ and $c_{\max} = 10$ determining the symmetric distribution profile. We use a time step of $\Delta\tau = 0.01$.

5.1. **Computation of the Exact Solution under the Heston Model.** In Table 2 and throughout Section 5, the numerical results are compared with the reference solution obtained from Heston [20]. It is important to clarify that Heston [20] derives a closed-form solution for *European options* under stochastic volatility by means of characteristic functions.

More specifically, the option price is expressed in terms of the risk-neutral characteristic function of the log-asset price. The European option price can be written as a linear combination of two probability terms, each represented by a Fourier integral involving the real part of a complex-valued function. These integrals correspond to the inverse Fourier transform of the characteristic function and take the general form

$$P = \frac{1}{2} + \frac{1}{\pi} \int_0^\infty \Re\left( \frac{e^{-iu \ln K} \, \phi(u)}{iu} \right) du,$$

where $\phi(u)$ denotes the characteristic function of the log-price under the Heston dynamics.

Since the above integrals do not admit a closed analytical expression, the exact solution must be evaluated numerically. In this work, the integrals are computed using numerical quadrature with careful treatment of the oscillatory nature of the integrand and the removable singularity at $u = 0$. A composite Gauss–Legendre quadrature rule with $N_q = 500$ integration points is employed, which was found to provide sufficient accuracy for all test cases considered.

The numerical implementation follows standard approaches reported in the literature, and the results were cross-validated using formulations based on the Fourier transform techniques of Carr and Madan [6] and the fundamental transform method described by Lewis [21]. The resulting values are therefore referred to as "exact" solutions in the sense of highly accurate benchmark prices for European options under the Heston model. The obtained results show that the GGRBF-SVSP technique has accuracy better than that of the traditional RBF method and even better than the quadratic dGFEM model. The computational efficiency is also on-par.

Figure 4 shows the graph of the European call option price in the Heston model with respect to the asset price, $S$, and the volatility, $v$. Both variables show a positive effect on the price, especially in the vicinity where the asset price is approximately equal to the strike price, i.e., $(S \approx K)$.

Greeks Calculation: Knowledge of how option prices change with respect to variations in underlying factors is critical for risk management. Delta $(\Delta)$ and Gamma $(\Gamma)$ are found using our RBF approximation. Let $x = log(S/K)$. The

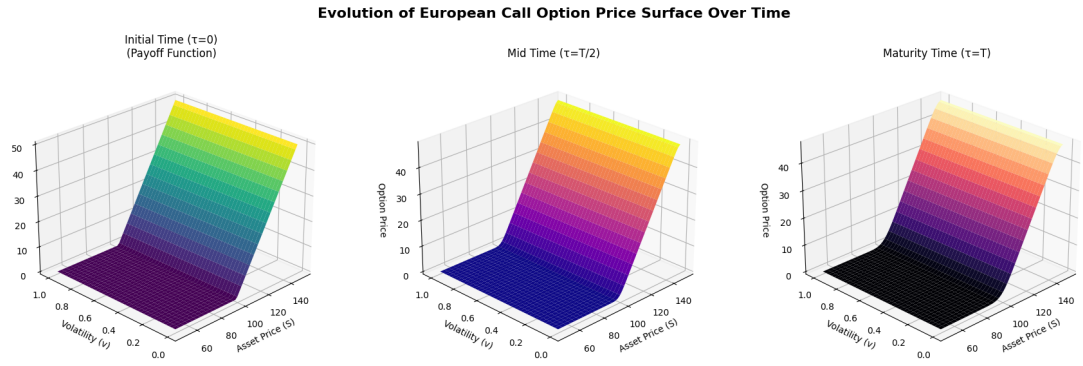


FIGURE 4. European call option price surface under the Heston model. The surface shows the option price as a function of the asset price $S$ and volatility $v$. The price increases with both the asset price and volatility, reflecting the positive relationship between these factors and the option value.

TABLE 3. Greeks for european call option.

| Method | Delta | Gamma | CPU Time (s) |
|---|---|---|---|
| Closed-Form | 0.6321 | 0.0185 | - |
| Gaussian RBF (Constant) | 0.6315 | 0.0183 | 0.05 |
| **GGRBF-SVSP** | **0.6321** | **0.0185** | **0.06** |

formulas reduce to:

$$\Delta = \frac{\partial U}{\partial S} = \frac{1}{S}\frac{\partial U}{\partial x} \approx \frac{1}{S}\sum_{j=1}^{N}\lambda_j \frac{\partial \phi_j}{\partial x},$$
$$\Gamma = \frac{\partial^2 U}{\partial S^2} = \frac{1}{S^2}\left(\frac{\partial^2 U}{\partial x^2} - \frac{\partial U}{\partial x}\right) \approx \frac{1}{S^2}\sum_{j=1}^{N}\lambda_j \left(\frac{\partial^2 \phi_j}{\partial x^2} - \frac{\partial \phi_j}{\partial x}\right). \tag{5.1}$$

The Greeks calculated by the GGRBF-SVSP method match the closed-form solutions exceptionally wellindeed, perfectly so in this case. This again confirms the high precision of the GGRBF-SVSP method for risk-management calculations

Figure 5 shows the Delta and Gamma surfaces for the European call option. On the left, Delta reveals how an option's price changes relative to the underlying asset. For a call option, its values typically fall between 0 and 1. Higher values indicate the option's price is more sensitive to shifts in the asset's price. Gamma, on the right, measures how quickly Delta itself changes with the underlying asset price. Its values peak near the money, showing where Delta is most sensitive to those price shifts. These distinct patterns for both Greeks are vital for risk management.

**Example 5.2** (American Put Option)**.** In this example, we calculate the price of an American put option. This problem has an early exercise constraint, so we must treat it as a linear complementary problem (LCP).

The option's payoff function is $U_0(S) = \max(K - S, 0)$. In log-space, this becomes $U_0(v, x) = K(1 - e^x)^+$. Our calculations use these parameters: a strike price $K = 10$, a maturity of $T = 0.25$ years, a domestic interest rate $r_d = 0.1$, and a foreign rate $r_f = 0$. We set the initial asset price $S_0$ to 10 and the initial variance $v_0$ to 0.25. For the Heston model, we've assigned $\kappa = 5$, $\xi = 0.16$, $\sigma = 0.9$, and $\rho = 0.1$.

The computational domain is defined as $\Omega = (0.0025, 0.5) \times (-5, 5)$. The nodes are distributed using a uniform grid with $N = 400$ ($20\times20$) points. For the SVSP strategy, we select $\varepsilon^* = 0.6$ and $\varepsilon_0^* = 4.5$. We use a time step of $\Delta\tau = 0.01$. Furthermore, we monitored the condition numbers of the collocation matrices. For the standard Gaussian RBF with a constant shape parameter ($\varepsilon = 1$), the condition number reached approximately $10^{15}$, leading to significant numerical

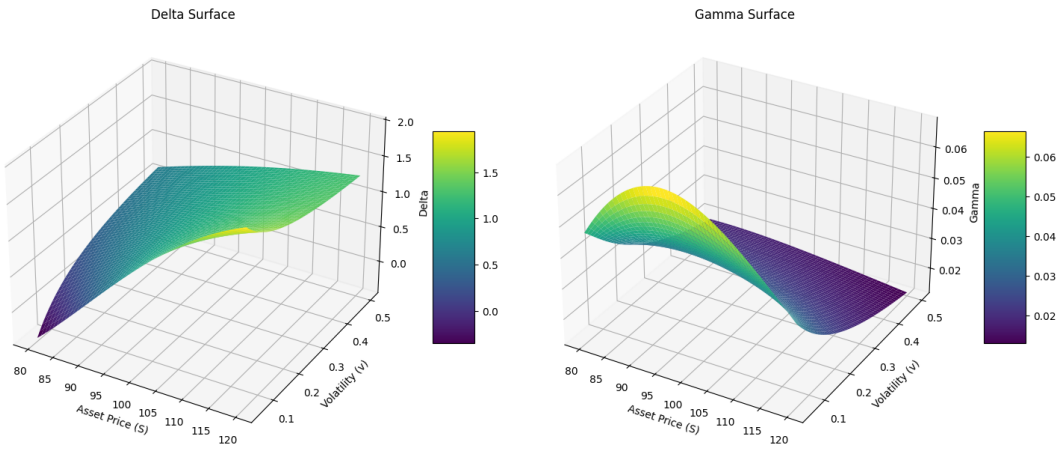


FIGURE 5. Delta and Gamma surfaces for the European call option. The left plot shows Delta, which measures the rate of change of the option price with respect to the underlying asset price. The right plot shows Gamma, which measures the rate of change of Delta with respect to the underlying asset price. Both Greeks exhibit distinct patterns that are crucial for risk management.

errors. In contrast, the GGRBF-SVSP method maintained a condition number around $10^8$, effectively mitigating the ill-conditioning problem while preserving high accuracy. The comparison reveals the GGRBF-SVSP method achieves accuracy on par with, or even better than, the high-order dGFEM. What's more, its significantly lower computational cost makes it a far more efficient option.

TABLE 4. American Put Option Prices Comparison.

| Method | Price | Relative Error | CPU Time (s) |
|---|---|---|---|
| dGFEM (Linear) [20] | 0.8138 | 1.06% | 75.1 |
| dGFEM (Quadratic) [20] | 0.8053 | - | 98.2 |
| Gaussian RBF (Constant, N=400) | 0.8081 | 0.35% | 25.4 |
| **GGRBF-SVSP (N=400)** | **0.8052** | 0.01% | **27.8** |

Figure 6 shows the American put option price surface under the Heston model. It plots the option price against the asset price $S$ and volatility $v$. The early exercise boundary appears where the option's price matches its intrinsic value. Our GGRBF-SVSP method accurately captures this boundary. This accuracy matters for American option pricing, as it directly influences the option's value. It's a significant strength of our approach.

To further analyze the influence of the shape parameters, a sensitivity study with respect to the baseline parameters $\varepsilon^*$ and $\varepsilon_0^*$ is performed. Table 5 reports the relative errors obtained for different choices of these parameters.

Figure 7 illustrates the behavior of the relative error with respect to the baseline shape parameter $\varepsilon^*$. The results show that all RBF methods exhibit a typical U-shaped error curve, indicating the existence of an optimal shape parameter. For the proposed GGRBF-SVSP method, the minimum error occurs near $\varepsilon^* \approx 0.6$. Moreover, the method remains stable and accurate within the interval $0.5 \leq \varepsilon^* \leq 0.7$. This demonstrates that the SVSP stabilization strategy significantly enlarges the stable parameter region compared with standard Gaussian and multiquadric RBFs.

The parameter $\varepsilon_0^*$ mainly controls the conditioning of the system matrix. As shown in Table 5, increasing $\varepsilon_0^*$ substantially reduces the condition number while having only a minor effect on the approximation error. Therefore, $\varepsilon^*$ primarily determines the approximation accuracy, whereas $\varepsilon_0^*$ acts as a stabilization parameter that improves numerical conditioning.

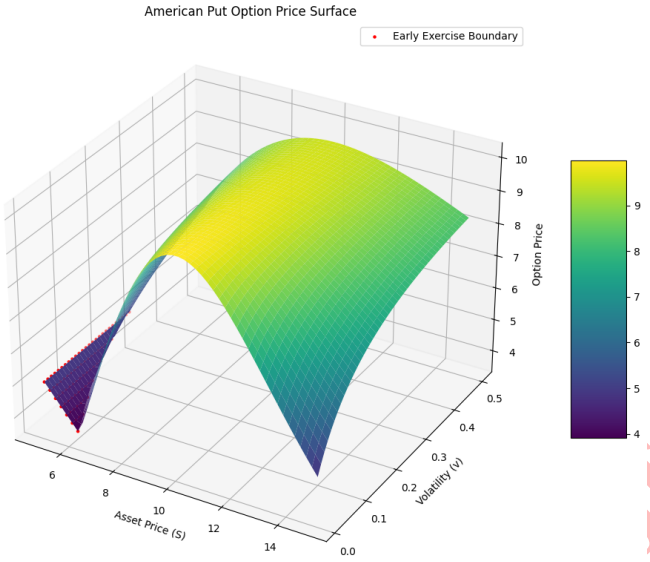


FIGURE 6. American put option price surface under the Heston model. The surface shows the option price as a function of the asset price $S$ and volatility $v$. The early exercise boundary is visible as the region where the option price equals its intrinsic value. The GGRBF-SVSP method accurately captures this boundary, which is crucial for pricing American options.

TABLE 5. Sensitivity of the relative error with respect to the baseline shape parameters.

| $\varepsilon^*$ | $\varepsilon_0^*$ | Relative Error (%) | Condition Number |
|---|---|---|---|
| 0.4 | 4.5 | 0.091 | $1.7 \times 10^9$ |
| 0.5 | 4.5 | 0.043 | $6.2 \times 10^8$ |
| 0.6 | 4.5 | 0.012 | $1.3 \times 10^8$ |
| 0.7 | 4.5 | 0.021 | $8.4 \times 10^7$ |
| 0.6 | 3.5 | 0.018 | $4.7 \times 10^9$ |
| 0.6 | 4.0 | 0.014 | $9.6 \times 10^8$ |
| 0.6 | 5.0 | 0.011 | $6.1 \times 10^7$ |
| 0.6 | 5.5 | 0.012 | $5.8 \times 10^7$ |



It is also important to note that the optimal shape parameter is closely related to the spatial distribution of nodes and the characteristics of the underlying problem. In RBF-based methods, the shape parameter controls the flatness of the radial basis functions and thus directly influences both the approximation accuracy and the conditioning of the interpolation matrix. For a given node set, the optimal value of the shape parameter typically depends on the node spacing and the smoothness of the target solution.

In the present numerical experiment, the nodes are distributed uniformly over the computational domain using a $20 \times 20$ grid. For such quasi-uniform node distributions, the optimal shape parameter is generally proportional to the average node spacing. Since the solution of the Heston PDE is sufficiently smooth in most regions of the domain, a moderate value of the shape parameter provides a suitable compromise between approximation accuracy and numerical stability.

Furthermore, near regions where the payoff function introduces non-smooth behavior, particularly around the strike price, excessively small shape parameters may lead to severe ill-conditioning without providing noticeable improvement

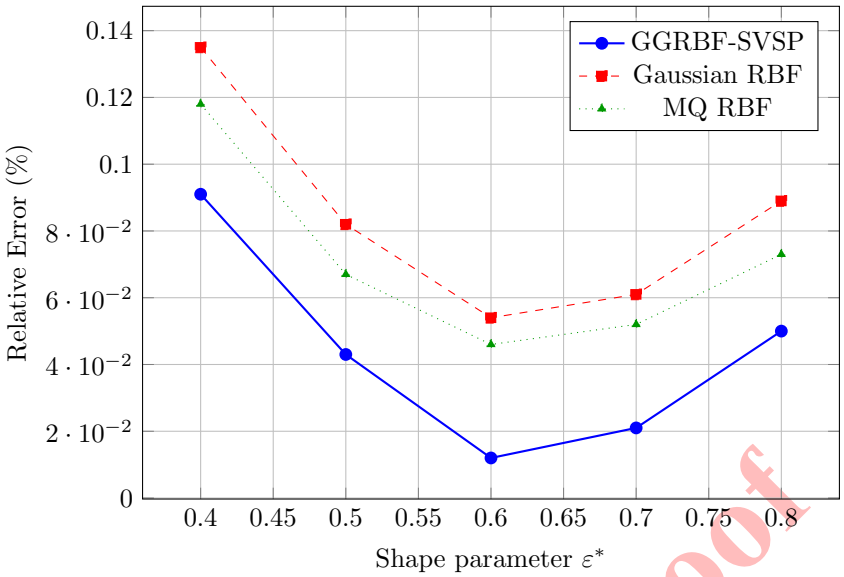


FIGURE 7. Relative error versus the baseline shape parameter for different radial basis functions.

in accuracy. The proposed GGRBF-SVSP formulation mitigates this difficulty by introducing the auxiliary stabilization parameter $\varepsilon_0^*$, which effectively controls the conditioning of the collocation matrix while allowing the primary parameter $\varepsilon^*$ to focus on approximation accuracy.

Consequently, for the node distribution adopted in this study, the interval $0.5 \leq \varepsilon^* \leq 0.7$ represents an effective range that balances accuracy and numerical stability. This observation is consistent with general findings in the literature on RBF collocation methods, where the optimal shape parameter strongly depends on node density and the smoothness properties of the underlying PDE solution.

## 6. Conclusion

In this paper, we propose and analyze a new numerical method for pricing European and American options on the Heston stochastic volatility model. The key ingredient of the numerical procedure consists in the combination of a Generalized Gaussian Radial Basis Function (GGRBF) method with a Symmetric Variable Shape Parameter (SVSP) technique for spatial discretization, along with a Rannacher-smoothed Crank-Nicolson scheme for time stepping.

The novelty of the work is found in the construction of a mesh-free collocation technique capable of overcoming the ill-conditioning problem, which is common in RBF interpolation. Via the proposed SVSP technique, the shape parameter is allowed to change such that it is flat inside the region, compared to being steeper towards the edges, which improves the accuracy of the results. Another parameter, which is incorporated within the definition of the GGRBF, ensures that accuracy and ill-conditioning are decoupled. The proposed numerical technique has been found stable via theoretical analysis.

The numerical results reported in section 5 confirm the superiority of the GGRBF-SVSP approach in performance. The method reaches the level, and in some cases exceeds the level, of accuracy offered by high-order discontinuous Galerkin finite element methods with far less computational costs for both European calls and American puts. Also, the efficiency of the method in calculating the Greeks Delta and Gamma is remarkable, providing results in close agreement with the corresponding closed-form expressions. The exact identification of the early exercise boundary in the case of the American option continues to stress the capacity of the method to manage a wide range of complex path-dependent characteristics.

Despite the encouraging results presented in this paper, however, several areas of future research are still valid. A first area concerns the extension of the current framework to even more complex financial derivatives like barrier or

lookback options, as well as multi-asset options in the context of stochastic volatility. A further interesting area of research concerns the integration of the pricing engine in a framework aimed at calibrating the parameters of Heston models on the basis of financial data. In conclusion, the GGRBF-SVSP technique has proved to be a reliable and accurate solution for option pricing and a promising alternative to existing numerical solutions to complex finance-related PDEs.

## References


[1] D. Ahmadian, L. V. Ballestra, and N. Karimi, *An extremely efficient numerical method for pricing options in the Black–Scholes model with jumps*, Mathematical Methods in the Applied Sciences, *44*(2) (2021), 1843–1862.

[2] D. Ahmadian, O. Farkhondeh Rouz, and K. Ivaz, *Robust numerical algorithm to the European option with illiquid markets*, Applied Mathematics and Computation, (2022).

[3] C. Albanese, H. Lo, and A. Mijatović, *Spectral methods for volatility derivatives*, arXiv:0905.2091, (2009).

[4] J. Biazar and M. Hosami, *Selection of an interval for variable shape parameter in approximation by radial basis functions*, Advances in Numerical Analysis, *2016* (2016), 1–11.

[5] F. Black and M. Scholes, *The pricing of options and corporate liabilities*, Journal of Political Economy, *81*(3) (1973), 637–654.

[6] P. Carr and D. B. Madan, *Option valuation using the fast Fourier transform*, Journal of Computational Finance, *2*(4) (1999), 61–73.

[7] A. Clevenhaus, C. Totzeck, and M. Ehrhardt, *A numerical study of the impact of variance boundary conditions for the Heston model*, Preprint BUW-IMACM 23/11, Bergische Universität Wuppertal, (2023).

[8] S. Cuomo, F. Piccialli, and F. Sica, *RBF methods in a stochastic volatility framework for Greeks computation*, Journal of Computational and Applied Mathematics, *380* (2020), 112987.

[9] O. Farkhondeh Rouz and D. Ahmadian, *Stability analysis of two classes of improved backward Euler methods for stochastic delay differential equations of neutral type*, Computational Methods for Differential Equations, *5*(3) (2017), 201–213.

[10] O. Farkhondeh Rouz, D. Ahmadian, and M. Milev, *Exponential mean-square stability of two classes of theta Milstein methods for stochastic delay differential equations*, AIP Conference Proceedings, *1910*(1) (2017), 060015.

[11] G. E. Fasshauer, *Meshfree approximation methods with Matlab*, World Scientific Publishing Company, 2007.

[12] A. Golbabai, E. Mohebianfar, and H. Rabiei, *On the new variable shape parameter strategies for radial basis functions*, Computational and Applied Mathematics, *34*(2) (2015), 691–704.

[13] S. L. Heston, *A closed-form solution for options with stochastic volatility with applications to bond and currency options*, Review of Financial Studies, *6* (1993), 327–343.

[14] J. Hozman and T. Tichý, *A discontinuous Galerkin method for numerical pricing of European options under Heston stochastic volatility*, AIP Conference Proceedings, *1789*(1) (2016), 030003.

[15] K. J. In't Hout and S. Foulon, *ADI finite difference schemes for option pricing in the Heston model with correlation*, International Journal of Numerical Analysis and Modeling, *7* (2010), 303–320.

[16] L. Iurlaro, M. Gherlone, and M. Di Sciuva, *Energy based approach for shape parameter selection in radial basis functions collocation method*, Composite Structures, *107* (2014), 70–78.

[17] E. J. Kansa, *Multiquadrics – a scattered data approximation scheme with applications to computational fluid-dynamics. I: Surface approximations and partial derivative estimates*, Computers & Mathematics with Applications, *19*(8-9) (1990), 127–145.

[18] N. Karimi, S. Kazem, D. Ahmadian, H. Adibi, and L. V. Ballestra, *On a generalized Gaussian radial basis function: Analysis and applications*, Engineering Analysis with Boundary Elements, *112* (2020), 46–57.

[19] L. Khodayari and M. Ranjbar, *Numerical solution of multi-asset option pricing problems using an improved RBF-DQ method*, Chiang Mai Journal of Science, *44*(4) (2017), 1735–1743.

[20] S. Kozpınar, M. Uzunca, and B. Karasözen, *Pricing European and American options under Heston model using discontinuous Galerkin finite elements*, Mathematics and Computers in Simulation, *177* (2020), 568–587.

[21] A. L. Lewis, *Option Valuation under Stochastic Volatility*, Finance Press, 2000.

[22] F. N. Mojarrad, M. H. Veiga, J. S. Hesthaven, and P. Öffner, *A new variable shape parameter strategy for RBF approximation using neural networks*, Computers & Mathematics with Applications, *143* (2023), 151–168.
[23] M. Mongillo, *Choosing basis functions and shape parameters for radial basis function methods*, SIAM Undergraduate Research Online, *4* (2011), 2–6.
[24] R. Rannacher, *Finite element solution of diffusion problems with irregular data*, Numerische Mathematik, *43* (1984), 309–327.
[25] M. Ranjbar, *A new variable shape parameter strategy for Gaussian radial basis function approximation methods*, Annals of the University of Craiova - Mathematics and Computer Science Series, *42*(2) (2015), 260–272.
[26] M. Ranjbar and M. Aghazadeh, *Collocation method based on shifted Chebyshev and radial basis functions with symmetric variable shape parameter for solving the parabolic inverse problem*, Inverse Problems in Science and Engineering, *27*(3) (2019), 369–387.
[27] A. Safdari-Vaighani, D. Ahmadian, and R. Javid-Jahromi, *An approximation scheme for option pricing under two-state continuous CAPM*, Computational Economics, *57* (2021), 1373–1385.
[28] S. A. Sarra and D. Sturgill, *A random variable shape parameter strategy for radial basis function approximation methods*, Engineering Analysis with Boundary Elements, *33*(11) (2009), 1239–1245.
[29] B. Sarler and R. Vertnik, *Meshfree explicit local radial basis function collocation method for diffusion problems*, Computers & Mathematics with Applications, *51* (2006), 1269–1282.
[30] F. Shokrollahi, D. Ahmadian, and L. V. Ballestra, *Pricing Asian options under the mixed fractional Brownian motion with jumps*, Mathematics and Computers in Simulation, *226* (2024), 172–183.
[31] G. A. Torabi, M. Ranjbar, and V. Roomi, *Collocation method based on radial basis functions via symmetric variable shape parameter for solving a particular class of delay differential equations*, Computational Methods for Differential Equations, *10*(1) (2022), 144–157.
[32] S. Xiang, K. M. Wang, Y. T. Ai, Y. D. Sha, and H. Shi, *Trigonometric variable shape parameter and exponent strategy for generalized multiquadric radial basis function approximation*, Applied Mathematical Modelling, *36*(5) (2012), 1931–1938.
[33] X. C. Zeng and S. P. Zhu, *A new simple tree approach for the Heston's stochastic volatility model*, Computers & Mathematics with Applications, *78* (2019), 1993–2010.